Charge distribution in plasmas with field constraint

F. Lado
Department of Physics, North Carolina State University, Raleigh, North Carolina 27695-8202

James W. Dufty
Department of Physics, University of Florida, Gainesville, Florida 32611

(Received 9 March 1987)

The charge distribution around an atom in a strongly coupled plasma is calculated for equilibrium states constrained to produce a specified electric field at the atom. It is shown that recently developed methods for electric microfield distributions can be applied directly to calculation of the charge distribution functions as well. Two such methods are considered: effective-field independent-particle models and integral equations with complex potential.

I. INTRODUCTION

The atomic and radiative properties of particles in plasmas are important for many applications in laser fusion, magnetic confinement, and astrophysical studies.[1] The local plasma environment can have a significant effect on these properties due to the long-range Coulomb interaction and high densities frequently encountered. A detailed microscopic analysis of such highly correlated systems is difficult, and it is often useful to formulate atomic calculations explicitly in terms of a few dominant properties of the plasma. In many cases the most important properties are the total electric field at the atom, and the average distribution of charges nearby. There are excellent theories available for calculation of the probability distribution of the electric microfields for a wide range of plasma conditions.[2] However, the presence of a given field value at the atom implies an anisotropic distribution of the local plasma charge density to produce such a field. This charge distribution is the usual pair correlation function for the atom and a plasma particle, except with equilibrium averages conditioned by the given electric field. The objectives here are threefold: first, to show that this conditional pair correlation function can be obtained directly from the theory for microfield distribution functions; second, to illustrate the quantitative effects of the field constraint on the charge distribution for strongly coupled plasmas; and third, to compare two different models currently used to calculate microfield distribution functions.

The joint probability density for the electric field at the atom to have the value $\boldsymbol{\varepsilon}$ and for a charge to be at position $\mathbf{r}$ relative to the atom is defined by

$$P(\mathbf{r},\boldsymbol{\varepsilon}) \equiv \langle n(\mathbf{r})\delta(\boldsymbol{\varepsilon}-\mathbf{E})\rangle \ . \tag{1}$$

Here the brackets denote an equilibrium average, $n(\mathbf{r})$ is the microscopic number density at $\mathbf{r}$, and $\mathbf{E}$ is the electric microfield due to the plasma. The conditional charge distribution $g(\mathbf{r};\boldsymbol{\varepsilon})$ is the probability density for a plasma particle at $\mathbf{r}$, given an atom at the origin in a microfield $\boldsymbol{\varepsilon}$,

$$P(\mathbf{r},\boldsymbol{\varepsilon}) \equiv Q(\varepsilon) n_0 g(\mathbf{r};\boldsymbol{\varepsilon}) \ , \tag{2}$$

where n_0 is the average charge density and $Q(\varepsilon)$ is the usual electric microfield distribution,

$$Q(\varepsilon) \equiv \langle \delta(\boldsymbol{\varepsilon}-\mathbf{E})\rangle \ . \tag{3}$$

Current theories for calculation of $Q(\varepsilon)$ are based on approximations to the corresponding generating functional $\tilde{Q}(\lambda)$,

$$Q(\varepsilon) \equiv \int \frac{d\boldsymbol{\lambda}}{(2\pi)^3} e^{-i\boldsymbol{\lambda}\cdot\boldsymbol{\varepsilon}} \tilde{Q}(\lambda) \ . \tag{4}$$

A useful representation for $\tilde{Q}(\lambda)$ has been given by Iglesias[3]

$$\ln\tilde{Q}(\lambda) = \int_0^\lambda dl \int d\mathbf{r}\, i\hat{\boldsymbol{\lambda}}\cdot\mathbf{E}(\mathbf{r}) n_0 \tilde{g}(\mathbf{r};l) \ , \tag{5}$$

where $\mathbf{E}(\mathbf{r})$ is the electric field due to a charge at $\mathbf{r}$ and $\hat{\boldsymbol{\lambda}}$ is the unit vector associated with $\boldsymbol{\lambda}$. This representation follows directly from the identity

$$\begin{aligned}\ln\tilde{Q}(\lambda) &= \int_0^\lambda dl \frac{\partial}{\partial l} \ln\tilde{Q}(l) \\ &= \int_0^\lambda dl\, i\hat{\boldsymbol{\lambda}}\cdot\langle \mathbf{E} e^{il\cdot\mathbf{E}}\rangle / \tilde{Q}(\lambda) \\ &= \int_0^\lambda dl \int d\mathbf{r}\, i\hat{\boldsymbol{\lambda}}\cdot\mathbf{E}(\mathbf{r})\langle n(\mathbf{r}) e^{il\cdot\mathbf{E}}\rangle / \tilde{Q}(\lambda) \ . \end{aligned} \tag{6}$$

Comparison of (6) and (5) gives the precise definition of $\tilde{g}(\mathbf{r};\mathbf{l})$,

$$n_0 \tilde{g}(\mathbf{r};l) = \langle n(\mathbf{r}) e^{il\cdot\mathbf{E}}\rangle / \langle e^{il\cdot\mathbf{E}}\rangle \ . \tag{7}$$

The function $\tilde{g}(\mathbf{r};\boldsymbol{\lambda})$ now can be interpreted[3] as the equilibrium pair correlation function for a fluid with complex potential energy, $U(\{\mathbf{r}_i\};\boldsymbol{\lambda}) = U(\{\mathbf{r}_i\}) - \beta^{-1} i\boldsymbol{\lambda}\cdot\mathbf{E}(\{\mathbf{r}_i\})$ where $U(\{\mathbf{r}_i\})$ is the usual interaction energy for the one-component plasma (OCP) and the atom, and β^{-1} is the temperature.

The main point of interest here is to recognize that $\tilde{g}(\mathbf{r};l)$ is also simply related to the constrained distribution function $g(\mathbf{r},\boldsymbol{\varepsilon})$, according to

$$Q(\varepsilon) g(\mathbf{r};\boldsymbol{\varepsilon}) = \int \frac{d\boldsymbol{\lambda}}{(2\pi)^3} \tilde{Q}(\lambda)\tilde{g}(\mathbf{r};\boldsymbol{\lambda}) \ . \tag{8}$$

The proof of (8) follows immediately from the definitions of $g(\mathbf{r};\varepsilon)$ and $Q(\varepsilon)$ in Eqs. (1)–(3). Equations (5) and (8) show that the function $\tilde{g}(\mathbf{r};\lambda)$ determines both $Q(\varepsilon)$ and $g(\mathbf{r};\varepsilon)$. Further analysis shows that higher-order constrained distribution functions also can be obtained from $\tilde{g}(\mathbf{r};\lambda)$ by suitable functional differentiation, so it is appropriate to consider $\tilde{g}(\mathbf{r};\lambda)$ as the primary theoretical quantity. Recently, simple models for $\tilde{g}(\mathbf{r};\lambda)$ have been applied for the calculation of $Q(\varepsilon)$, with results that are accurate over a wide range of plasma conditions including strong coupling.[2] Two of these approximations are extended in Sec. II to calculate $g(\mathbf{r};\varepsilon)$. The first is an independent-particle model with an effective-field [adjustable-parameter exponential approximation[4] (APEX)], while the second is an application of integral-equation methods.[5]

Before discussing these models, we note two exact moment conditions for $g(\mathbf{r};\varepsilon)$,[6]

$$\int d\varepsilon\, Q(\varepsilon) g(\mathbf{r};\varepsilon) = g(r) \tag{9}$$

$$\int d\varepsilon\, Q(\varepsilon)\varepsilon g(\mathbf{r};\varepsilon) = \mathbf{E}_{\mathrm{MF}}(r) g(\mathbf{r}) , \tag{10}$$

where $g(r)$ is the usual equilibrium radial distribution function and $\mathbf{E}_{\mathrm{MF}}$ is the "mean force field,"

$$e\mathbf{E}_{\mathrm{MF}}(\mathbf{r}) \equiv \beta^{-1}\nabla \ln g(r) . \tag{11}$$

The proof of (9) and (10) is straightforward and will not be given here. It is also possible to show that (9) and (10) will be satisfied if

$$\tilde{g}(\mathbf{r};l)\,|_{l=0} = g(r) , \tag{12}$$

$$-i\frac{d}{dl}\tilde{g}(\mathbf{r};l)\,|_{l=0} = \mathbf{E}_{\mathrm{MF}}(\mathbf{r}) g(r) , \tag{13}$$

respectively. Further comment on these conditions is given in the discussion section.

The conditional charge distribution $g(\mathbf{r};\varepsilon)$ has been evaluated previously in the weak-coupling limit.[7] Also, Greene has calculated a related distribution for an idealized noninteracting plasma.[8] The connection with this latter case is given in Sec. IV.

II. TWO MODELS

Consider a system consisting of an atom (charged or neutral) immersed in a plasma. To simplify the discussion attention is restricted to a classical one-component plasma and the internal degrees of freedom of the atom are suppressed. The more general case of a multicomponent, quantum plasma follows in an obvious manner. The equilibrium configuration is specified by the center-of-mass position of the atom, $\mathbf{r}_0$, and the positions of the plasma particles relative to the atom, $\{\mathbf{r}_i\}$. Two types of models have been suggested for calculation of $Q(\varepsilon)$ from approximations to $\tilde{g}(\mathbf{r};\lambda)$.

A. Independent-particle models

This class of models is defined by the approximation

$$\tilde{g}(\mathbf{r};\lambda) \to g(r) e^{i\lambda\cdot\mathbf{E}^*(\mathbf{r})} , \tag{14}$$

where the effective field $\mathbf{E}^*(r)$ is independent of λ. The resulting microfield distribution then has the same form as that for a fluid of independent particles, interacting only with atoms at the origin,

$$\ln\tilde{Q}(\lambda) = n\int d\mathbf{r}\, g^*(r)(e^{i\lambda\cdot\mathbf{E}^*(r)} - 1) . \tag{15}$$

Here $g^*(r)$ is an effective charge density for the independent particles related to $g(r)$ by

$$\mathbf{E}^*(\mathbf{r}) g^*(r) = \mathbf{E}(\mathbf{r}) g(r) . \tag{16}$$

Equation (16) leads to the natural interpretation[4] of $g^*(r)$ as the appropriate charge density for $\mathbf{E}^*(r)$ to produce the exact local field at $\mathbf{r}$. The choice of $\mathbf{E}^*(r)$ is constrained by the requirement that the second moment of $Q(\varepsilon)$ be exact, but is otherwise arbitrary. The corresponding conditional charge distribution is obtained directly from substitution of (14) into (8),

$$g(\mathbf{r};\varepsilon)/g(r) = Q[\varepsilon - \mathbf{E}^*(\mathbf{r})]/Q(\varepsilon) , \tag{17}$$

where it is understood that the microfield distributions on the right-hand side of (17) are the independent-particle model functions. This is a particularly simple result that shows that $g(\mathbf{r};\varepsilon)$ can be obtained directly from the strict equilibrium distributions, $Q(\varepsilon)$ and $g(r)$. One choice for $\mathbf{E}^*(\mathbf{r})$, known as APEX,[4] is a Debye-Hückel field,

$$\mathbf{E}^*_{\mathrm{APEX}}(\mathbf{r}) = \mathbf{E}(\mathbf{r})(1+\alpha r)e^{-\alpha r} , \tag{18}$$

where the screening length α^{-1} is determined by the second moment of $Q(\varepsilon)$.

B. Integral-equation models

These models are based on the interpretation of $\tilde{g}(\mathbf{r};\lambda)$ as an equilibrium pair correlation function for a fluid with complex potential energy, as indicated following Eq. (7). This interpretation suggests the extension of well-developed integral-equation methods for equilibrium correlation functions.[9] The basic approach is to solve an associated Ornstein-Zernike equation for $h(\mathbf{r};\lambda) \equiv \tilde{g}(\mathbf{r};\lambda) - 1$,

$$h(\mathbf{r};\lambda) = c(\mathbf{r};\lambda) + n_0\int d\mathbf{r}'\, h(\mathbf{r}';\lambda) c(\mathbf{r}-\mathbf{r}';0) , \tag{19}$$

together with a closure relation,

$$c(\mathbf{r};\lambda) = h(\mathbf{r};\lambda) - \ln\{\tilde{g}(\mathbf{r};\lambda)\exp[\beta\phi(r) - i\lambda\cdot\mathbf{E}(\mathbf{r})]\} + B(\mathbf{r};\lambda) . \tag{20}$$

The model is defined by an approximation to the generalized "bridge function," $B(\mathbf{r};\lambda)$. Recent studies of this method have shown that very accurate microfield distributions can be obtained from the approximation,[5]

$$B(\mathbf{r},\lambda) = B_{\mathrm{HS}}(r) + \frac{i\lambda\cdot\hat{\mathbf{r}}}{\beta e}\frac{d}{dr}B_{\mathrm{HS}}(r) . \tag{21}$$

Here, $B_{\mathrm{HS}}(r)$ is the bridge function for a fluid of hard spheres. A more detailed outline of the algorithm for solution of Eqs. (19)–(21) is given in Ref. 5. With $\tilde{g}(\mathbf{r};\lambda)$ determined in this way, $Q(\varepsilon)$ and $g(\mathbf{r};\varepsilon)$ can be computed from (4), (5), and (8). The λ integration is performed using a Legendre polynomial expansion to get

$$g(\mathbf{r};\boldsymbol{\varepsilon})=\sum_{l=0}^{\infty} G_l(r,\varepsilon)P_l(\cos\theta)\ ,$$

$$G_l(r,\varepsilon)\equiv\frac{(-1)^l}{2\pi^2 i^{l+\sigma}}\int_0^\infty d\lambda\,\lambda^2\tilde{Q}(\lambda)\tilde{g}_l(r,\lambda)j_l(\lambda\varepsilon)/Q(\varepsilon)\ , \tag{22}$$

where $\sigma=0$ for l even and $\sigma=1$ for l odd, $j_l(x)$ is the spherical Bessel function, and $\tilde{g}_l(r,\lambda)$ are the coefficients in the Legendre polynomial expansion of $\tilde{g}(\mathbf{r};\boldsymbol{\lambda})$. The sum in (22) is found to be rapidly convergent.

III. RESULTS

The charge distribution is a function of three variables: the magnitudes of $\mathbf{r}$ and $\boldsymbol{\varepsilon}$ and the angle between these vectors, θ,

$$g(\mathbf{r};\boldsymbol{\varepsilon})\equiv g(r,\varepsilon,\theta)\ . \tag{23}$$

The qualitative behavior of $g(r,\varepsilon,\theta)$ is easily anticipated. For fixed ε,θ, the charge distribution is small at small r (due to short-range repulsion), has a peak near the interparticle separation, $r_0=(3/4\pi n_0)^{1/3}$, and approaches unity for large r. Next, for given r,ε, there will be an excess of charges at $\theta=\pi$ and a depletion at $\theta=0$, in order to produce the field $\boldsymbol{\varepsilon}$. Finally, as ε is increased this difference between $\theta=0$ and $\theta=\pi$ is enhanced.

To illustrate these properties of $g(\mathbf{r};\boldsymbol{\varepsilon})$ we first apply the integral-equation method to the case of equal charge for the atom and plasma particles, at a plasma parameter of $\Gamma=\beta e^2/r_0=10$. This represents a strongly coupled plasma, well outside the Debye-Hückel domain. Figure 1 shows $g(r,\varepsilon,\theta)$ for $\varepsilon/\varepsilon_0=0.2$ ($\varepsilon_0\equiv e/r_0^2$) as a function of r/r_0 at $\theta=0$, $\pi/2$, π. Figures 2 and 3 show the same quantities at $\varepsilon/\varepsilon_0=0.4$ and $\varepsilon/\varepsilon_0=0.8$, respectively. [The distribution of field values, $4\pi\varepsilon^2 Q(\varepsilon)$, has a maximum at about $\varepsilon/\varepsilon_0=0.4$ for this value of Γ.] At the lowest field value, Fig. 1, and $\theta=\pi/2$ the location and magnitude of the peak are similar to that for the unconstrained $g(r)$. As expected, for $\theta=\pi$ the peak is shifted toward the origin and increased, while for $\theta=0$, the opposite effect is observed. These distortions of $g(r)$ are enhanced as the field is increased to its average value, Fig. 2, and are quite dramatic at twice the average value, Fig. 3. We conclude that the field-constrained charge distribution differs significantly, both qualitatively and quantitatively, from the isotropic equilibrium distribution.

Next we consider a comparison of these results with those obtained from the independent-particle model, (17), using the APEX field (18). As for the previous results, the equilibrium pair correlation function is calculated using an optimized reference hypernetted chain approximation.[10]. Figure 4 shows the results for $\varepsilon/\varepsilon_0=0.4$ at $\theta=0$, $\pi/2$, and π. The expected qualitative features are observed, but a comparison with the corresponding results from the integral equation method in Fig. 2 shows large differences. This is somewhat unexpected since both methods agree closely when used to calculate $Q(\varepsilon)$. To understand the reason for the differences here, consider the moment conditions (9) and (10). If the equivalent conditions (12) and (13) are substituted into the Ornstein-Zernicke equation (19) and the closure approximation (21), it can be shown (see Appendix) that the integral-equation method satisfies both moment conditions. The independent-particle models also satisfy (9), but the field moment result is

$$\int d\boldsymbol{\varepsilon}\,Q(\varepsilon)\boldsymbol{\varepsilon}g(\mathbf{r},\boldsymbol{\varepsilon})=\mathbf{E}^*(\mathbf{r})g(r)\ . \tag{24}$$

Thus the independent-particle models satisfy (10) only if $\mathbf{E}^*(\mathbf{r})$ is chosen to be the mean force field $\mathbf{E}_{\rm MF}$, or a good approximation to it. This is not the case for $\mathbf{E}^*_{\rm APEX}$, as is shown in Table I.[11] The APEX field differs from the mean force field by as much as 100% over the relevant

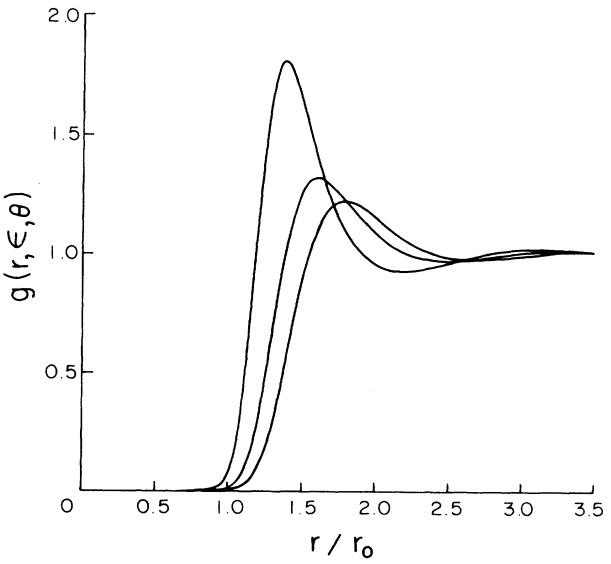

FIG. 1. $g(r,\varepsilon,\theta)$ calculated by the integral-equation method for $\Gamma=10$, $\varepsilon/\varepsilon_0=0.2$. Top curve is for $\theta=\pi$, middle curve is for $\theta=\pi/2$, and lower curve is for $\theta=0$.

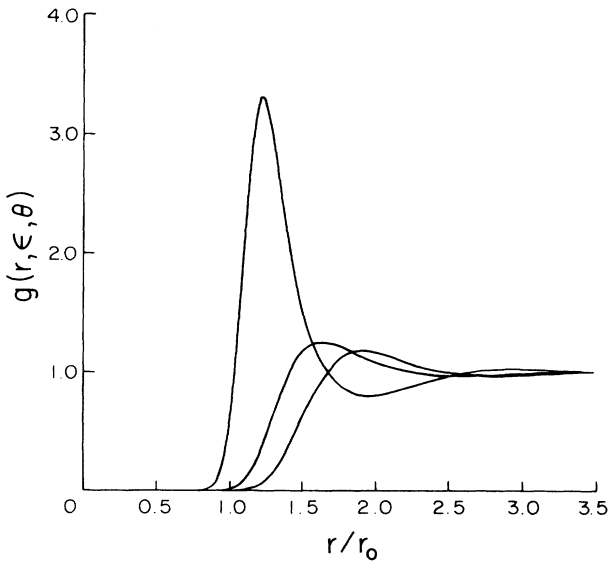

FIG. 2. Same as Fig. 1 for $\varepsilon/\varepsilon_0=0.4$.

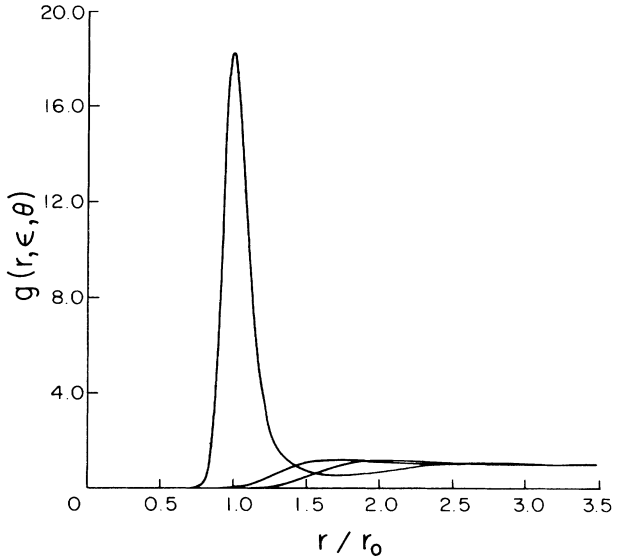

FIG. 3. Same as Fig. 1 for $\varepsilon/\varepsilon_0=0.8$.

range of r, and this can introduce large errors in the APEX $g(\mathbf{r};\boldsymbol{\varepsilon})$. This suggests that, although both the integral equation and APEX methods are reliable for calculation of $Q(\varepsilon)$, the former is probably more accurate for calculation of $g(\mathbf{r};\boldsymbol{\varepsilon})$. Further evidence from computer simulation would be desirable.

It might be thought that the relative simplicity of the independent-particle model result, (17), could be maintained if $\mathbf{E}^*(r)$ were chosen to be $\mathbf{E}_{\rm MF}(r)$ instead of $\mathbf{E}_{\rm APEX}$, so that condition (10) is satisfied. In fact, this choice has been used recently to calculate $Q(\varepsilon)$ with good results in moderately coupled plasmas.[12] However, it appears that $\mathbf{E}_{\rm MF}(\mathbf{r})$ is an inappropriate choice for the strongly coupled conditions considered here. The problem arises because $\mathbf{E}_{\rm MF}(\mathbf{r})$ is oscillatory at large Γ. Consequently, when $\hat{\mathbf{r}}\cdot\mathbf{E}_{\rm MF}$ changes sign an unphysical sign change in the effective charge density of Eq. (16) is also implied. [A systematic derivation of the independent-particle models[13] also fails due to a singularity in the renormalization transformation when $\hat{\mathbf{r}}\cdot\mathbf{E}^*$ changes sign; see Eq. (4.2) of Ref. 13.] It appears that the mean force field is not a suitable choice in the independent-particle models for very strongly coupled plasmas.

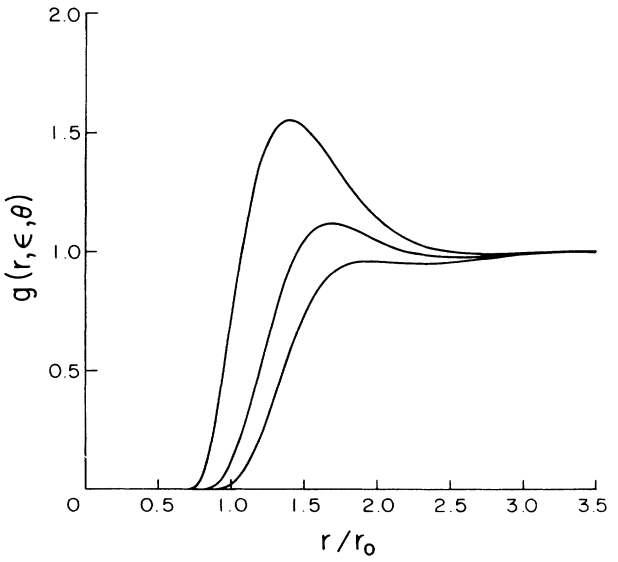

FIG. 4. $g(r,\varepsilon,\theta)$ calculated by the APEX method for $\Gamma=10$, $\varepsilon/\varepsilon_0=0.4$.

TABLE I. Comparison of $E^*_{\rm APEX}$ and $E_{\rm MF}$.

r/r_0	$E^*_{\rm APEX}$	$E_{\rm MF}$
0.503	2.78	3.74
0.604	1.72	2.48
0.704	1.11	1.71
0.805	0.742	1.21
1.01	0.356	0.616
1.21	0.182	0.301
1.41	0.097	0.109
1.71	0.0398	−0.0122
1.81	0.0299	−0.0251
2.01	0.0170	−0.0274
2.21	0.0100	−0.0152

IV. DISCUSSION

To indicate one application of the conditional charge distribution, consider the spectral line broadening of atomic radiation. Most spectral line-broadening theories treat the perturbing ions as static during the relevant radiation times, and consider the atom in a fixed field $\boldsymbol{\varepsilon}$ due to the ions. In the dipole approximation this field entirely characterizes the atom-plasma interaction. However, if higher-order multipole effects are important, the conditional charge distribution is also required. For a simple one-electron ion, the appropriate average energy of interaction with the OCP is

$$\langle V\rangle_{\varepsilon}\equiv\langle V\delta(\boldsymbol{\varepsilon}-\mathbf{E})\rangle_0/Q(\varepsilon)\ , \tag{25}$$

$$V=\sum_i\left[zV(\mathbf{r}_i)-V(\mathbf{r}_i-\mathbf{r}_a)\right]$$

$$=\int d\mathbf{r}\,V(r)[zn(\mathbf{r})-n(\mathbf{r}+\mathbf{r}_a)]\ . \tag{26}$$

Here, $V(r)$ is the Coulomb potential, ze is the nuclear charge, and $\mathbf{r}_a$ is the atomic electron coordinate relative to the nucleus. Substitution of (2) into (25) gives

$$\langle V\rangle_{\varepsilon}=n_0\int d\mathbf{r}\,V(r)[zg(\mathbf{r};\boldsymbol{\varepsilon})-g(\mathbf{r}+\mathbf{r}_a;\boldsymbol{\varepsilon})]\ . \tag{27}$$

The atomic matrix elements for states of interest can be calculated in a Fourier representation. Previous calculations of this average interaction have typically neglected the dependence of the distribution on the field ε.[14] The results of Sec. III indicate this is a questionable approximation.

It was noted at the end of the Introduction that Greene has recently calculated a related quantity.[8] Specifically, he considers the joint probability density of the *nearest* charge to be at $\mathbf{r}$, and the field due to the remaining

charges to be ε. This probability density can be written in a form analogous to (1),

$$\bar{P}(\mathbf{r},\varepsilon)=\langle n(\mathbf{r})\delta[\varepsilon+\mathbf{E}(\mathbf{r})-\mathbf{E}]\rangle_r \ , \tag{28}$$

where $\mathbf{E}$ is again the total microscopic field due to the plasma and $\mathbf{E}(\mathbf{r})$ is the field due to a charge at $\mathbf{r}$. The brackets $\langle\ \rangle_r$ now denote an equilibrium average with the potential energy for interaction between the atom and plasma, $V(\{r_i\})$, replaced by

$$V(r,\{r_i\})=\begin{cases} V(\{r_i\}), & \text{all } r_i>r \\ \infty, & \text{any } r_i<r \ . \end{cases} \tag{29}$$

The hard core assures that the charge at r is the nearest charge. It is then easily seen that the representations (4), (6), and (8) apply with $\varepsilon\rightarrow\varepsilon+\mathbf{E}(\mathbf{r})$, and the models of Sec. II can be used for this problem as well. In this way the ideal gas calculations of Greene can be extended easily to strongly coupled plasmas.

ACKNOWLEDGMENTS

The authors are indebted to David Boercker and Carlos Iglesias for helpful comments and suggestions. This research was supported by National Science Foundation Grant Nos. CHE-84-11932 and CHE-84-02144.

APPENDIX: MOMENT CONDITIONS ON $g(\mathbf{r};\varepsilon)$

The moment conditions on $g(\mathbf{r};\varepsilon)$ are calculated here for the independent-particle models and the integral-equation models. It is convenient to study these conditions in the forms (12) and (13) for $\tilde{g}(\mathbf{r};\boldsymbol{\lambda})$.

1. Independent-particle models

In this case $\tilde{g}(\mathbf{r},\boldsymbol{\lambda})$ is given by the approximation (14), which leads directly to

$$\tilde{g}(\mathbf{r};\boldsymbol{\lambda})\,|_{\lambda=0}=g(r) \ ,$$
$$i\frac{d\tilde{g}}{d\lambda}(\mathbf{r};\boldsymbol{\lambda})\,|_{\lambda=0}=-E^*(\mathbf{r})g(r) \ . \tag{A1}$$

Therefore, the zeroth moment condition is always satisfied, but the first moment condition holds only if $\mathbf{E}^*(\mathbf{r})=\mathbf{E}_{\mathrm{MF}}(r)$.

2. Integral-equation models

The integral-equation methods are defined by Eqs. (19)–(21). For $\lambda=0$ these equations yield $g(r)$ exactly if the exact bridge function is used. An optimized hard-sphere bridge function produces an excellent approximation to $g(r)$.[10] To study the first moment condition, differentiate the Ornstein-Zernicke equation with respect to λ. Then it follows that the exact condition (13) holds only if

$$i\frac{\partial c}{\partial\lambda}(\mathbf{r};\boldsymbol{\lambda})\,|_{\lambda=0}=-(e\beta)^{-1}\frac{\partial c}{\partial r}(\mathbf{r};0) \ . \tag{A2}$$

Next, differentiate Eq. (20) for $c(r;\lambda)$ to find that (A2) holds only if

$$i\frac{\partial B}{\partial\lambda}(\mathbf{r};\boldsymbol{\lambda})=-(e\beta)^{-1}\frac{\partial B}{\partial r}(\mathbf{r};0) \ . \tag{A3}$$

Thus Eq. (A3) is an equivalent statement of the first moment condition in terms of the quantity that defines a particular integral-equation model. For the choice here, Eq. (21), the condition (A3) is clearly satisfied.

[1]See, for example, *Strongly Coupled Plasmas, NATO Advanced Study Institute Series B: Physics,* edited by H. deWitt and F. Rogers (Plenum, New York, 1987).
[2]For a recent review with references, see J. W. Dufty in *Strongly Coupled Plasmas,* Ref. 1.
[3]C. Iglesias, Phys. Rev. A **27**, 2705 (1983).
[4]C. Iglesias, J. Lebowitz, and D. MacGowan, Phys. Rev. A **28**, 1667 (1983).
[5]F. Lado, in *Strongly Coupled Plasmas,* Ref. 1; Phys. Rev. A **34**, 4131 (1986); **36**, 313 (1987).
[6]D. Boercker (private communication).
[7]C. Iglesias and J. Dufty, in *Spectral Line Shapes,* edited by K. Burnett (W. De Gruyter, New York, 1983), Vol. 2.
[8]R. Greene, Phys. Rev. A **34**, 4091 (1986).
[9]J. P. Hansen and I. R. McDonald, *Theory of Simple Liquids* (Academic, New York, 1976).
[10]F. Lado, S. M. Foiles, and N. W. Ashcroft, Phys. Rev. A **28**, 2374 (1983).
[11]The mean force field is calculated in two steps. First, $\ln g(r)$ is determined as in Ref. 10 and then the space derivative is calculated by a second-order finite-difference method.
[12]A. Alastuey, C. Iglesias, J. Lebowitz, and D. Levesque, Phys. Rev. A **30**, 2537 (1984); X.-Z. Yan and S. Ichimaru, *ibid.* **34**, 2167 (1986).
[13]J. W. Dufty, D. B. Boercker, and C. Iglesias, Phys. Rev. A **31**, 1681 (1985).
[14]The importance of constrained charge distributions for spectral line shifts has been noted by C. Iglesias, Phys. Rev. A **29**, 1366 (1984). The field dependence of the quadrupole interaction energy has been estimated using a nearest-neighbor approximation: R. Joyce, L. Woltz, and C. F. Hooper, Jr., Phys. Rev. A **35**, 2228 (1987).